J. Phys. Earth, **30**, 1–31, 1982

HIGHER MOMENT EXCITATION OF NORMAL MODES AND SURFACE WAVES

Emile A. OKAL

Department of Geology and Geophysics, Yale University, New Haven, Connecticut, U.S.A.

(Received September 9, 1981)

Following the formalism introduced initially by Backus and Malcuhy, and developed for body waves by Stump, we investigate the excitation of normal modes and surface waves in the Earth by higher moments, characteristic of seismic sources with extended lateral dimensions. We derive coefficients of excitation in the most general case for second order moments (third-order tensors), and show that they can be readily computed from the double-couple excitation coefficients for all geometries, and for both normal modes and surface waves. We apply our results to a number of simple fault models, including ruptures involving vertical propagation, which cannot be treated by the classic directivity method. While it is in principle possible to correct for the vertical extent of the source through the use of the centroidal double-couple in the case of simple ruptures, our formalism can be applied to any geometry. Our results show that vertical rupture, even over short distances (10 km), can substantially modify the excitation of normal modes in the case of dip-slip sources. This may have important consequences for moment tensor inversion, and in the search for deep lateral heterogeneities. Finally, this formalism may be transposed to the theory of tsunami generation.

1. *Introduction*

In order to retrieve information about seismic sources and structures, it has been common use in the past 15 years to make use of synthetic seismograms. In the case of surface waves, this approach has been particularly successful since the work of HARKRIDER (1964), who showed that one could conveniently separate excitation from propagation. Since then, Green's function responses for point body forces have been obtained and converted for point-source double-couples, notably in the case of surface waves by HARKRIDER (1964, 1970), and for normal modes by SAITO (1967), GILBERT (1970), and KANAMORI and CIPAR (1974). In the case of large earthquakes, for which the dimensions and duration of the source cannot be neglected, one is then led to the following expression for the k-th component of the displacement $\boldsymbol{u}$ at location $\boldsymbol{x}$ and time t:

$$u_k(\boldsymbol{x}, t)=\int_{-\infty}^{\infty} \mathrm{d}\tau \int_V G_{ik}(\boldsymbol{x}, t; \boldsymbol{\xi}, \tau) f_i(\boldsymbol{\xi}, \tau) \mathrm{d}^3\boldsymbol{\xi} \,, \tag{1}$$

where $\boldsymbol{f}(\boldsymbol{\xi}, \tau)$ is the density of force acting at point $\boldsymbol{\xi}$ and time τ and G_{ik} the Green's function response. V is the volume of the source, which only has to be bounded. For a buried fault contained in the plane $\xi_3=0$, $\boldsymbol{f}$ is given in terms of the seismic slip $[\Delta \boldsymbol{u}]$ in the plane of faulting by:

$$\boldsymbol{f}(\boldsymbol{\xi}, \tau) = -\mu(\boldsymbol{\xi})[\Delta \boldsymbol{u}(\boldsymbol{\xi}, \tau)] \frac{\partial}{\partial \xi_3} \delta(\xi_3) - \mathrm{div}_2\{\mu(\boldsymbol{\xi})[\Delta \boldsymbol{u}(\boldsymbol{\xi}, \tau)]\} \delta(\xi_3) \hat{\boldsymbol{e}}_3 \,, \tag{2}$$

where μ is the medium's rigidity, div_2 denotes the divergence operator in the plane $\xi_3=0$, and $\hat{\boldsymbol{e}}_3$ is the unit vector normal to this plane (AKI and RICHARDS, 1980). Assuming knowledge of the function $[\Delta \boldsymbol{u}]$ in space and time, one is faced, in computing integral (1), with several options:

a. An actual numerical computation of the integral. Although this procedure is in principle always possible, it is lengthy and can be very expensive, because it requires the computation of many different Green's functions, for various combinations of x and $\boldsymbol{\xi}$.

b. One can try to obtain a simple analytic expansion of the integral, assuming the slip history $[\Delta \boldsymbol{u}(\boldsymbol{\xi}, \tau)]$ itself to have a simple analytic form. This approach, named directivity theory, was introduced by BEN-MENAHEM (1961) and has been widely used in the study of large earthquakes. However, it has several shortcomings: in order to obtain an integral calculable analytically, one has to meet three conditions: a simple expression for $[\Delta \boldsymbol{u}]$, a simple expression for G, and a simple shape for the faulting area. The second condition, for example, restricts its use for normal modes to the range of distances where asymptotic expansions of the Legendre functions are valid; at low angular orders, this may be a strong constraint.

c. An other approach, introduced originally by BACKUS and MULCAHY (1976), is to expand G in a Taylor's series of $\boldsymbol{\xi}$, about a reference point $\boldsymbol{\xi}=\boldsymbol{0}$, thereby taking G out of the integral, and leaving a much more manageable source integral. Specifically, one writes:

$$G_{ik}(x, t; \boldsymbol{\xi}, \tau) = \sum_{n=0}^{\infty} \frac{1}{n!} \xi_{j_1} \xi_{j_2} \cdots \xi_{j_n} G_{ik, j_1 j_2 \cdots j_n}(x, t; \boldsymbol{0}, \tau) \,, \tag{3}$$

$$M_{i j_1 j_2 \cdots j_n}(t) = \int_V \xi_{j_1} \xi_{j_2} \cdots \xi_{j_n} f_i(\boldsymbol{\xi}, t) \mathrm{d}^3 \boldsymbol{\xi} \tag{4}$$

and then one merely has:

$$u_k(x, t) = \sum_{n=0}^{\infty} \frac{1}{n!} G_{ik, j_1 j_2 \cdots j_n}(x, t; \boldsymbol{0}, 0) \otimes M_{i j_1 j_2 \cdots j_n}(t) \,. \tag{5}$$

The M's are the moments of the system of forces $\boldsymbol{f}$ about the point $\boldsymbol{\xi}=\boldsymbol{0}$, commas denote derivatives with respect to $\boldsymbol{\xi}$, and the symbol $\otimes$ indicates convolution.

This method was applied to body waves by STUMP (1978), up to order $n=3$. Its main drawback is the number of terms needed, rapidly growing with the size of the source (the convergence of the series was discussed by BACKUS and MULCAHY

(1976)). However, it has many advantages: first, it is a linear method, and as such holds potential for use in inversion theory; also, it can be readily applied to any source geometry and time function, however complex they may be. It is interesting to note that the classic results concerning excitation of body waves, surface waves and normal modes by double-couples or more generally second-order moment tensors, are indeed an application of this method to order $n=1$ (the term $n=0$ is always zero, since the resultant of all internal forces vanishes identically).

The purpose of this paper is to derive excitation coefficients of the Earth's normal modes and surface waves, for the most general system of sources in the case $n=2$, and to discuss some of their properties and applications. In this paper, the symbol n will always be the order of the Taylor's series in formulae (3, 4, 5); we will refer to the corresponding moments as being of order $(n+1)$, since they are $(n+1)$-index tensor, although they actually represent the n-th moment of the system of forces $\boldsymbol{f}$.

2. *Excitation of Normal Modes by Third-Order Moments* ($n=2$)

2.1 *Introduction*

We will consider a normal mode of the Earth (which at this point can be either toroidal or spheroidal) and denote its angular order by l, its azimuthal order by m, and its overtone index by N. We will write the set $\{N, l, m\}$ as the superscript index $^\circ$. Let $\boldsymbol{u}^\circ$ be its displacement eigenfunction, ω° and Q° its angular frequency and attenuation; it is well known (GILBERT, 1970) that its excitation by a system of forces with density $\boldsymbol{f}(\boldsymbol{\xi})$ and step-function time dependence is:

$$A^\circ(t)=\frac{1}{I}\int_V \boldsymbol{u}^\circ(\boldsymbol{\xi})\cdot\boldsymbol{f}(\boldsymbol{\xi})\mathrm{d}^3\boldsymbol{\xi}\,\frac{1-\cos\omega^\circ t\exp(-\omega^\circ t/2Q^\circ)}{(\omega^\circ)^2}\,, \tag{6}$$

where the normalizing factor $I=\int\rho(\boldsymbol{\xi})[\boldsymbol{u}^\circ(\boldsymbol{\xi})]^2\mathrm{d}^3\boldsymbol{\xi}$ can be assumed to be one, and will be dropped. Here ρ is the local density in the Earth, and V the volume of the planet. In this way, the displacement resulting from $\boldsymbol{f}$ at any point $\boldsymbol{x}$ is written:

$$\boldsymbol{u}(\boldsymbol{x}, t)=\sum_\circ A^\circ(t)\boldsymbol{u}^\circ(\boldsymbol{x})\,, \tag{7}$$

or, in terms of Green's functions:

$$G^\circ_{ik}(\boldsymbol{x}, t; \boldsymbol{\xi}, 0)=u_i{}^\circ(\boldsymbol{\xi})u_k{}^\circ(\boldsymbol{x})\,\frac{1-\cos\omega^\circ t\exp(-\omega^\circ t/2Q^\circ)}{(\omega^\circ)^2}\,. \tag{8}$$

It is straightforward to apply this result to a first-order moment ($n=1$) leading to the well-known formula for the excitation of normal modes by a second-order symmetric tensor with step-function time dependence applied at $\boldsymbol{\xi}$:

$$\boldsymbol{u}(\boldsymbol{x}, t)=\sum_\circ \varepsilon^\circ_{ij}(\boldsymbol{\xi})M_{ij}\,\boldsymbol{u}^\circ(\boldsymbol{x})\,\frac{1-\cos\omega^\circ t\exp(-\omega^\circ t/2Q^\circ)}{(\omega^\circ)^2}\,, \tag{9}$$

where ε is simply the eigenstrain of each mode.

Generalizing to higher orders of moments, we obtain:

$$\boldsymbol{u}(\boldsymbol{x}, t)=\sum_{\circ} \boldsymbol{u}^{\circ}(\boldsymbol{x}) \sum_{n=1}^{\infty} \frac{1}{n!} u^{\circ}_{i, j_1 j_2 \cdots j_n}(\boldsymbol{x}_s) \dot{M}_{i j_1 j_2 \cdots j_n} \otimes \frac{1-\cos \omega^{\circ} t \exp \left(-\omega^{\circ} t / 2 Q^{\circ}\right)}{(\omega^{\circ})^2} . \quad (10)$$

Here, we have written $\boldsymbol{x}_s$ for the origin of the $\hat{\xi}$ frame, which will be the point at which the moments are computed; the rapid computation of the terms in Eq. (10) requires only cataloguing the derivatives making up the "superstrain" tensor $u_{i, j_1 j_2 \cdots j_n}$. We shall now concentrate on one mode (and therefore drop the superscript °), and obtain expressions of the excitation coefficients in the notation of KANAMORI and CIPAR (1974), which has the advantage of being readily usable when the geographic parameters of the earthquake source are known. However, we will consider simultaneously all members of a multiplet (same N, same l, different m), since individual components of source tensors can excite several of them. Thus, following OKAL and GELLER (1979), we will define excitation coefficients in which summation over m has been carried out. Specifically, and in the case of spheroidal modes, these authors introduced coefficients A_{ij} such that the term $\sum_{\circ} [\varepsilon^{\circ}_{ij} M_{ij} / (\omega^{\circ})^2] u_r^{\circ}(\boldsymbol{x})$ in Eq. (9), and for the vertical component of motion, could be simply written $-2 \sum_{N, l} A_{ij} M_{ij}$, A_{ij} including the (θ, ϕ) dependence in $\boldsymbol{x}$. (The factor -2 is designed to facilitate the passage to the frequency domain, since the term $-\cos \omega^{\circ} t$ in Eq. (9) will yield $-(1/2) e^{i \omega^{\circ} t}$.) Our purpose will be to obtain the set of coefficients E_{ijk} such that $A_{ij} M_{ij}$ should be supplemented at order $n=2$ by $(1/2!) E_{ijk} M_{ijk}$. In the case of toroidal modes, and for the azimuthal component of motion, we will similarly seek a different set of coefficients E_{ijk}, such that OKAL and GELLER's (1979) $B_{ij} M_{ij}$ is supplemented by $(1/2!) E_{ijk} M_{ijk}$.

2.2 *Toroidal modes*

Following SAITO (1967), we write the displacement of the mode ${}_N T_l^m$:

$$\left.\begin{aligned} u_r(r, \theta, \phi) &= 0 \\ u_\theta(r, \theta, \phi) &= m \frac{y_1(r)}{\sin \theta} P_l^m(\cos \theta) \operatorname{sc}(m \phi) \\ u_\phi(r, \theta, \phi) &= -y_1(r) \frac{\mathrm{d} P_l^m}{\mathrm{d} \theta} \operatorname{cs}(m \phi) . \end{aligned}\right\} \quad (11)$$

Here, we have used

$$\operatorname{cs}(\phi)=\begin{bmatrix} \cos \phi \\ \sin \phi \end{bmatrix} \quad \text{and} \quad \operatorname{sc}(\phi)=\begin{bmatrix} -\sin \phi \\ \cos \phi \end{bmatrix},$$

so that $\operatorname{cs}'(\phi)=\operatorname{sc}(\phi)$ and $\operatorname{sc}'(\phi)=-\operatorname{cs}(\phi)$. Upper and lower solutions are both acceptable, but when we compute $\boldsymbol{u}(\hat{\boldsymbol{\xi}})$ and its derivatives as $\hat{\boldsymbol{\xi}}$ moves to the axis of spherical polars, we need to have $\theta \to 0$ and $\phi \to 0$ in order to keep continuity of the local frame of coordinates, and so all sines will vanish. Our problem is now to compute the limits of the 18 independent components of $w_{ijk}=u_{i, jk}$ as $\theta \to 0$, $\phi \to 0$, and $r \to r_s$. The Appendix gives the expression of the "superstrain" w in

spherical polars; we also make use of the following expansions for the P_l^m's in the vicinity of $\theta=0$:

$$P_l^m(\cos\theta)=a_{lm0}\theta^m+\theta^{m+2}\left[a_{lm1}-\frac{3l-2m}{6}a_{lm0}\right]+O(\theta^{m+4}) \tag{12}$$

with

$$a_{lmr}=\frac{(-1)^r(l+m)!}{2^{2r+m}r!(r+m)!(l-m-2r)!}\,,$$

readily derived from the classic formula (MORIGUCHI *et al.*, 1959):

$$P_l^m(\cos\theta)=\sum_{r=0}^{[(l-m)/2]}a_{lmr}\sin^{2r+m}\theta\cos^{l-2r-m}\theta\,. \tag{13}$$

Once these limits are obtained through somewhat extensive but otherwise straightforward algebra, we express the results in terms of the eigenvector $[y_1(r), y_2(r)]$ introduced by Saito, and renormalize them in the convention of KANAMORI and CIPAR (1974). We also carry out the summation over m, and the choice of sin or cos $m\phi$. For first order moments ($n=1$), we obtain

$$\left.\begin{aligned}
B_{rr}&=0\\
B_{r\theta}&=-\frac{L_2}{2}Q_1\sin\phi\\
B_{r\phi}&=\frac{L_2}{2}Q_1\cos\phi\\
B_{\theta r}&=\frac{L_1+L_2}{2}Q_1\sin\phi\\
B_{\theta\theta}&=\frac{L_2}{4}Q_2\sin 2\phi\\
B_{\theta\phi}&=-\frac{L_2}{4}Q_2\cos 2\phi\\
B_{\phi r}&=-\frac{L_1+L_2}{2}Q_1\cos\phi\\
B_{\phi\theta}&=-\frac{L_2}{4}Q_2\cos 2\phi\\
B_{\phi\phi}&=-\frac{L_2}{4}Q_2\sin 2\phi\,.
\end{aligned}\right\} \tag{14}$$

In the case of symmetric second-order tensors, these formulae reduce to OKAL and GELLER's (1979) expressions after summation of the non-diagonal elements (a typographical error in the sign of $B_{r\phi}$ is corrected). Also, we have used the notation $Q_m=\mathrm{d}P_l^m(\cos\theta)/\mathrm{d}\theta$. For third-order tensors ($n=2$), we find:

$$\left.\begin{aligned}
E_{rrr}&=0\\
E_{rr\theta}&=-\frac{L_1}{2r_s}\sin\phi Q_1
\end{aligned}\right.$$

$$
\begin{aligned}
E_{r r \phi} &= \frac{L_1}{2r_s} \cos \phi Q_1 \\
E_{r \theta \theta} &= -\frac{L_2}{2r_s} \sin 2\phi Q_2 \\
E_{r \theta \phi} &= \frac{L_2}{2r_s} \cos 2\phi Q_2 \\
E_{r \phi \phi} &= \frac{L_2}{2r_s} \sin 2\phi Q_2 \\
E_{\theta r r} &= -\left[L_1/r_s + \frac{L_2}{2r_s} (\omega^2 r_s^2/\beta^2 - L^2 + 2) \right] \sin \phi Q_1 \\
E_{\theta r \phi} &= -\frac{L_1}{4r_s} [L^2 Q_0 + \cos 2\phi Q_2] \\
E_{\theta r \theta} &= \frac{L_1}{4r_s} \sin 2\phi Q_2 \\
E_{\theta \theta \theta} &= \frac{L_1}{2r_s} \sin \phi Q_1 - \frac{L_2}{8r_s} [M^2 \sin \phi Q_1 - \sin 3\phi Q_3] \\
E_{\theta \theta \phi} &= -\frac{L_2}{8r_s} [M^2 \cos \phi Q_1 + \cos 3\phi Q_3] \\
E_{\theta \phi \phi} &= \frac{L_1}{2r_s} \sin \phi Q_1 - \frac{L_2}{8r_s} [3M^2 \sin \phi Q_1 + \sin 3\phi Q_3] \\
E_{\phi r r} &= \left[L_1/r_s + \frac{L_2}{2r_s} (\omega^2 r_s^2/\beta^2 - L^2 + 2) \right] \cos \phi Q_1 \\
E_{\phi r \theta} &= \frac{L_1}{4r_s} [L^2 Q_0 - \cos 2\phi Q_2] \\
E_{\phi r \phi} &= -\frac{L_1}{4r_s} \sin 2\phi Q_2 \\
E_{\phi \theta \theta} &= -\frac{L_1}{2r_s} \cos \phi Q_1 + \frac{L_2}{8r_s} [3M^2 \cos \phi Q_1 - \cos 3\phi Q_3] \\
E_{\phi \theta \phi} &= \frac{L_2}{8r_s} [M^2 \sin \phi Q_1 - \sin 3\phi Q_3] \\
E_{\phi \phi \phi} &= -\frac{L_1}{2r_s} \cos \phi Q_1 + \frac{L_2}{8r_s} [M^2 \cos \phi Q_1 + \cos 3\phi Q_3] \, .
\end{aligned}
\tag{15}
$$

In order to simplify the writing, we have set $Q_m = (\mathrm{d}P_l^m/\mathrm{d}\theta)(\cos\theta)$, $L^2 = l(l+1)$, and $M^2 = L^2 - 2$. The table must also be completed through the obvious relation $E_{\alpha\beta\gamma} = E_{\alpha\gamma\beta}$. The coefficients L_1 and L_2 are the ones defined by KANAMORI and CIPAR (1974). It is important to note that their knowledge is sufficient for the computation of all the E's.

2.3 Spheroidal modes

The situation is very similar. We write:

$$\left.\begin{aligned} u_r(r,\theta,\phi)&=y_1(r)P_l^m(\cos\theta)\mathrm{cs}(m\phi)\\ u_\theta(r,\theta,\phi)&=y_3(r)\frac{\mathrm{d}P_l^m}{\mathrm{d}\theta}(\cos\theta)\mathrm{cs}(m\phi)\\ u_\phi(r,\theta,\phi)&=my_3(r)\frac{1}{\sin\theta}P_l^m(\cos\theta)\mathrm{sc}(m\phi)\,, \end{aligned}\right\} \tag{16}$$

and again make use of the expressions for the superstrain w given in the Appendix, and of the general notation and normalization convention of KANAMORI and CIPAR (1974). For second-order tensors ($n=1$), we have:

$$\left.\begin{aligned} A_{rr}&=\frac{1}{6}[K_0+N_0]P_l^0\\ A_{r\theta}&=-\left[\frac{K_0-2N_0}{6}+\frac{M^2}{2}K_2\right]P_l^1\cos\phi\\ A_{r\phi}&=-\left[\frac{K_0-2N_0}{6}+\frac{M^2}{2}K_2\right]P_l^1\sin\phi\\ A_{\theta r}&=-\left[\frac{K_1}{2}-\frac{K_0-2N_0}{6}-\frac{M^2}{2}K_2\right]P_l^1\cos\phi\\ A_{\theta\theta}&=\frac{2N_0-K_0}{12}P_l^0-\frac{K_2}{4}P_l^2\cos 2\phi\\ A_{\theta\phi}&=-\frac{K_2}{4}P_l^2\sin 2\phi\\ A_{\phi r}&=-\left[\frac{K_1}{2}-\frac{K_0-2N_0}{6}-\frac{M^2}{2}K_2\right]P_l^1\sin\phi\\ A_{\phi\theta}&=-\frac{K_2}{4}P_l^2\sin 2\phi\\ A_{\phi\phi}&=\frac{2N_0-K_0}{12}P_l^0+\frac{K_2}{4}P_l^2\cos 2\phi\,, \end{aligned}\right\} \tag{17}$$

where we have used the notation $L^2=l(l+1)$; $M^2=L^2-2$. Again, and for symmetric tensors, these expressions would reduce to OKAL and GELLER's (1979) formulae (15). For third-order tensors ($n=2$), one obtains:

$$\left.\begin{aligned} E_{rrr}&=\left[-K_0-\frac{\lambda}{\lambda+2\mu}L^2K_2-\frac{\lambda+\mu}{\lambda+2\mu}L^2K_1+\left(\frac{L^2\lambda}{\lambda+2\mu}+\frac{\omega^2r^2}{\alpha^2}\right)K_4\right]\frac{P_l^0}{2r}\\ E_{rr\theta}&=[K_1+K_5]\frac{P_l^1}{2r}\cos\phi\\ E_{rr\phi}&=[K_1+K_5]\frac{P_l^1}{2r}\sin\phi\\ E_{r\theta\theta}&=\left[K_5+\frac{L^2+2}{2}K_4-L^2K_2\right]\frac{P_l^0}{2r}-K_6\frac{P_l^2}{4r}\cos 2\phi\\ E_{r\theta\phi}&=-K_6\frac{P_l^2}{4r}\sin 2\phi \end{aligned}\right\}$$

$$
\left.
\begin{aligned}
E_{r\phi\phi}&=\left[K_5+\frac{L^2+2}{2}K_4-L^2K_2\right]\frac{P_l^0}{2r}+K_6\frac{P_l^2}{4r}\cos 2\phi\\
E_{\theta rr}&=\left[-\frac{\lambda+\mu}{\mu}N_0+2K_1-\left(M^2-\frac{\omega^2r^2}{\beta^2}\right)K_2\right]\frac{P_l^1}{2r}\cos\phi\\
E_{\theta r\theta}&=\left[K_5-\frac{M^2}{2}K_4+\frac{L^2}{2}K_1\right]\frac{P_l^0}{2r}+[K_4-K_1]\frac{P_l^2}{4r}\cos 2\phi\\
E_{\theta r\phi}&=[K_4-K_1]\frac{P_l^2}{4r}\sin 2\phi\\
E_{\theta\theta\theta}&=\left[-K_6-K_1+\frac{3M^2}{4}K_2\right]\frac{P_l^1}{2r}\cos\phi-K_2\frac{P_l^3}{8r}\cos 3\phi\\
E_{\theta\theta\phi}&=\left[-K_6+\frac{M^2}{4}K_2\right]\frac{P_l^1}{2r}\cos\phi-K_2\frac{P_l^3}{8r}\sin 3\phi\\
E_{\theta\phi\phi}&=\left[K_6-K_1+\frac{M^2}{4}K_2\right]\frac{P_l^1}{2r}\cos\phi+K_2\frac{P_l^3}{8r}\cos 3\phi\\
E_{\phi rr}&=\left[-\frac{\lambda+\mu}{\mu}N_0+2K_1-\left(M^2-\frac{\omega^2r^2}{\beta^2}\right)K_2\right]\frac{P_l^1}{2r}\sin\phi\\
E_{\phi r\theta}&=[K_4-K_1]\frac{P_l^2}{4r}\sin 2\phi\\
E_{\phi r\phi}&=\left[K_5-\frac{M^2}{2}K_4+\frac{L^2}{2}K_1\right]\frac{P_l^0}{2r}-[K_4-K_1]\frac{P_l^2}{4r}\cos 2\phi\\
E_{\phi\theta\theta}&=\left[K_6-K_1+\frac{M^2}{4}K_2\right]\frac{P_l^1}{2r}\sin\phi-K_2\frac{P_l^3}{8r}\sin 3\phi\\
E_{\phi\theta\phi}&=\left[-K_6+\frac{M^2}{4}K_2\right]\frac{P_l^1}{2r}\cos\phi+K_2\frac{P_l^3}{8r}\cos 3\phi\\
E_{\phi\phi\phi}&=\left[-K_6-K_1+\frac{3M^2}{4}K_2\right]\frac{P_l^1}{2r}\sin\phi+K_2\frac{P_l^3}{8r}\sin 3\phi\,,
\end{aligned}
\right\}
\tag{18}
$$

where we introduce the following additional notation:

$$
\left.
\begin{aligned}
K_4&=\frac{K_0-2N_0}{6}+\frac{L^2}{2}K_2\\
K_5&=\frac{K_0+N_0}{3}\\
K_6&=K_4-K_2\,,
\end{aligned}
\right\}
\tag{19}
$$

and the quantities r, λ, μ pertain to the source ($\boldsymbol{x}=\boldsymbol{x}_s$; $\boldsymbol{\xi}=\mathbf{0}$). Again, although these formulae may appear complex, they only require the knowledge of the four excitation coefficients N_0, K_0, K_1, K_2 (or equivalently of the vector $[y_1, y_2, y_3, y_4]$) characteristic of second-order tensor excitation. In particular, the coefficients K_4, K_5, K_6 have been introduced only to ease the writing. We must note, however, that the relationship between the K's and the y's, as derived by Kanamori and Cipar and used in Eqs. (17) and (18), assumes that the influence of gravity can be

neglected, and that the degree of the differential system is reduced to 4. We shall come back to this problem in Sec. 6.4.

3. *Excitation of Surface Waves by Third-Order Moments* ($n=2$)

3.1 *Introduction*

By analogy with the normal mode problem, we will define in this section coefficients D_{ij} (at order $n=1$) and F_{ijk} (at order $n=2$) such that the resulting motion of the Earth's surface can be written:

$$u_*(\boldsymbol{x}, t)=\sum_N \int_0^\infty y_1(z)e^{i\omega t}\left[D_{ij}\dot{M}_{ij}(\omega)+\frac{1}{2}F_{ijk}\dot{M}_{ijk}(\omega)\right]d\omega \\ \{+\text{complex conjugate for } \omega<0\}\,. \tag{20}$$

In the case of Love waves, u_* will represent the transverse component u_ϕ; in the case of Rayleigh waves, it will be the vertical component u_z. N represents a summation over all overtone branches, which will be dropped from now on.

3.2 *Love waves*

In the case of Love waves, the eigenfunction $y_1(z)$ is such that the seismic displacement can be written:

$$\left.\begin{aligned} u_r(r, \phi, z; \omega)&=\frac{1}{kr}mJ_m(kr)\mathrm{sc}(m\phi)y_1(z)\\ u_\phi(r, \phi, z; \omega)&=-J_m'(kr)\mathrm{cs}(m\phi)y_1(z)\\ u_z(r, \phi, z; \omega)&=0 \end{aligned}\right\} \tag{21}$$

in a cylindrical frame of reference running through $\boldsymbol{x}=\boldsymbol{x}_s(\boldsymbol{\xi}=\boldsymbol{0})$. We then compute the strain and superstrain in cylindrical polars (see Appendix) and use the expansion

$$J_\nu(z)=(z/2)^\nu\sum_{p=0}^{\infty}\frac{(-z^2/4)^p}{p!(\nu+p)!} \tag{22}$$

to obtain their limits as $r\to 0$, $\phi\to 0$, $z\to z_s$. By comparison with Saito, and after defining the coefficients L_1^* and L_2^*:

$$L_2^*=y_1/8\pi C^2UI_1^L;\qquad L_1^*=y_2/8\pi C^2UI_1^L\mu k\,, \tag{23}$$

we obtain at order $n=1$:

$$\left.\begin{aligned} D_{rr}&=\frac{1}{2}L_2^*Q_2\sin 2\phi\\ D_{r\phi}&=-\frac{1}{2}L_2^*[Q_0+Q_2\cos 2\phi]\\ D_{rz}&=L_1^*Q_1\sin\phi \end{aligned}\right\}$$

$$\left.\begin{aligned} D_{\phi r} &= \frac{1}{2} L_2^* [Q_0 - Q_2 \cos 2\phi] \\ D_{\phi\phi} &= -\frac{1}{2} L_2^* Q_2 \sin 2\phi \\ D_{\phi z} &= -L_1^* Q_1 \cos \phi \\ D_{zr} &= 0 \\ D_{z\phi} &= 0 \\ D_{zz} &= 0 \end{aligned}\right\} \tag{24}$$

in which we have written $Q_m = [H_m^{(2)}]'(kr)$. (The passage from J_m to $H_m^{(2)}$ results from symmetry relations in (20)). Finally, in the case $n=2$, we obtain, with the same notation:

$$\left.\begin{aligned} F_{rrr} &= -\frac{kL_2^*}{4} [\sin \phi Q_1 - \sin 3\phi Q_3] \\ F_{r\phi r} &= -\frac{kL_2^*}{4} [\cos \phi Q_1 + \cos 3\phi Q_3] \\ F_{rzr} &= \frac{kL_1^*}{2} \sin 2\phi Q_2 \\ F_{\phi rr} &= \frac{kL_2^*}{4} [3 \cos \phi Q_1 - \cos 3\phi Q_3] \\ F_{\phi\phi r} &= \frac{kL_2^*}{4} [\sin \phi Q_1 - \sin 3\phi Q_3] \\ F_{\phi zr} &= \frac{kL_1^*}{2} [Q_0 - \cos 2\phi Q_2] \\ F_{zrr} &= 0 \\ F_{z\phi r} &= 0 \\ F_{zrz} &= 0 \\ F_{rz\phi} &= -\frac{kL_1^*}{2} [Q_0 + \cos 2\phi Q_2] \\ F_{rzz} &= kL_2^* [1 - C^2/\beta^2] \sin \phi Q_1 \\ F_{\phi z\phi} &= -\frac{kL_1^*}{2} \sin 2\phi Q_2 \\ F_{\phi zz} &= -kL_2^* [1 - C^2/\beta^2] \cos \phi Q_1 \\ F_{z\phi z} &= 0 \\ F_{zzz} &= 0 \\ F_{r\phi\phi} &= -\frac{kL_2^*}{4} [3 \sin \phi Q_1 + \sin 3\phi Q_3] \\ F_{\phi\phi\phi} &= \frac{kL_2^*}{4} [\cos \phi Q_1 + \cos 3\phi Q_3] \\ F_{z\phi\phi} &= 0 \,. \end{aligned}\right\} \tag{25}$$

3.3 Rayleigh waves

Similarly, in the case of Rayleigh waves, we write the seismic displacement as:

$$\left.\begin{aligned} u_r(r,\phi,z;\omega) &= y_3(z)J_m'(kr)\mathrm{cs}(m\phi) \\ u_\phi(r,\phi,z;\omega) &= m\frac{y_3(z)}{kr}J_m(kr)\mathrm{sc}(m\phi) \\ u_z(r,\phi,z;\omega) &= y_1(z)J_m(kr)\mathrm{cs}(m\phi)\ . \end{aligned}\right\} \tag{26}$$

In the notation of SAITO (1967), we introduce the following coefficients:

$$\left.\begin{aligned} K_1^* &= y_4/8\pi C^2 U I_1^R k\mu \\ K_2^* &= y_3/8\pi C^2 U I_1^R \\ K_3^* &= y_2/8\pi C^2 U I_1^R k\mu \\ K_4^* &= y_1/8\pi C^2 U I_1^R \end{aligned}\right\} \tag{27}$$

and obtain at order $n=1$:

$$\left.\begin{aligned} D_{rr} &= \frac{1}{2}K_2^*[Q_0 - Q_2\cos 2\phi] \\ D_{r\phi} &= -\frac{1}{2}K_2^* Q_2 \sin 2\phi \\ D_{rz} &= [K_4^* - K_1^*]Q_1 \cos\phi \\ D_{\phi r} &= -\frac{1}{2}K_2^* Q_2 \sin 2\phi \\ D_{\phi\phi} &= \frac{1}{2}K_2^*[Q_0 + Q_2\cos 2\phi] \\ D_{\phi z} &= [K_4^* - K_1^*]Q_1 \sin\phi \\ D_{zr} &= -K_4^* Q_1 \cos\phi \\ D_{z\phi} &= -K_4^* Q_1 \sin\phi \\ D_{zz} &= -\left[\frac{\lambda}{\lambda+2\mu}K_1^* + \frac{\mu}{\lambda+2\mu}K_3^*\right]Q_0 \end{aligned}\right\} \tag{28}$$

and at order $n=2$:

$$\left.\begin{aligned} F_{rrr} &= \frac{k}{4}K_2^*[3Q_1\cos\phi - Q_3\cos 3\phi] \\ F_{rr\phi} &= \frac{k}{4}K_2^*[Q_1\sin\phi - Q_3\sin 3\phi] \\ F_{rrz} &= -\frac{k}{2}[K_4^* - K_1^*][Q_0 - Q_2\cos 2\phi] \\ F_{r\phi\phi} &= \frac{k}{4}K_2^*[Q_1\cos\phi + Q_3\cos 3\phi] \\ F_{r\phi z} &= \frac{k}{2}[K_4^* - K_1^*]Q_2\sin 2\phi \end{aligned}\right\}$$

$$
\begin{aligned}
F_{rzz} &= k\left[\frac{\lambda+\mu}{\lambda+2\mu}(K_3^*-2K_2^*)-\left(1-\frac{C^2}{\beta^2}\right)K_2^*\right]Q_1\cos\phi \\
F_{\phi rr} &= \frac{k}{4}K_2^*[Q_1\sin\phi-Q_3\sin 3\phi] \\
F_{\phi r\phi} &= \frac{k}{4}K_2^*[Q_1\cos\phi+Q_3\cos 3\phi] \\
F_{\phi rz} &= \frac{k}{2}[K_4^*-K_1^*]Q_2\sin 2\phi \\
F_{\phi\phi\phi} &= \frac{k}{4}K_2^*[3Q_1\sin\phi+Q_3\sin 3\phi] \\
F_{\phi\phi z} &= -\frac{k}{2}[K_4^*-K_1^*][Q_0+Q_2\cos 2\phi] \\
F_{\phi zz} &= k\left[\frac{\lambda+\mu}{\lambda+2\mu}(K_3^*-2K_2^*)-\left(1-\frac{C^2}{\beta^2}\right)K_2^*\right]Q_1\sin\phi \\
F_{zrr} &= \frac{k}{2}K_4^*[Q_0-Q_2\cos 2\phi] \\
F_{zr\phi} &= -\frac{k}{2}K_4^*Q_2\sin 2\phi \\
F_{zrz} &= -k\left[\frac{\lambda}{\lambda+2\mu}K_2^*+\frac{\mu}{\lambda+2\mu}K_3^*\right]Q_1\cos\phi \\
F_{z\phi\phi} &= \frac{k}{2}K_4^*[Q_0+Q_2\cos 2\phi] \\
F_{z\phi z} &= -k\left[\frac{\lambda}{\lambda+2\mu}K_2^*+\frac{\mu}{\lambda+2\mu}K_3^*\right]Q_1\sin\phi \\
F_{zzz} &= k\left[\frac{\lambda+\mu}{\lambda+2\mu}(2K_4^*-K_1^*)-\left(1-\frac{C^2}{\alpha^2}\right)K_4^*\right]Q_0\,.
\end{aligned}
\tag{29}
$$

In these sets of formulae, we have put $Q_m=H_m^{(2)}(kr)$, k is the wavenumber, C the phase velocity, and the quantities λ, μ, α, β pertain to the source ($z=z_s$).

4. *Properties of the E's and F's*

In this section, we review a number of properties of the coefficients E_{ijk} and F_{ijk}, defined and computed in Secs. 2 and 3.

4.1 Asymptotic behavior and equivalence between the E's and the F's

Although the E's were specifically derived in order to be used in cases when asymptotic expansion of normal mode eigenfunctions is not warranted, it is important to check that the E's and F's become equivalent as we go asymptotically from normal modes to surface waves. This check can be best described on an example. Take the case of the toroidal mode coefficient

$$E_{\theta r\theta}=\frac{L_1}{4r_s}\sin 2\phi\,\frac{\mathrm{d}P_l^2}{\mathrm{d}\theta}(\cos\theta)$$

and of its Love counterpart

$$F_{rzr}=\frac{kL_1^*}{2}\sin 2\phi[H_2^{(2)}]'(kr)\ ;$$

let $l\to\infty$, $r_s/a\to 1$, $l/ak\to 1$, $l\sin\theta/kr\to 1$, replace $\sum_l$ by $\int(a/U)\mathrm{d}\omega$, and observe that $a^2I_1^L$ (Love)/I_1 (toroidal modes)$\to 1$ for similar normalization of the solution (e.g., $y_1(a)=1$ at the surface), so that

$$\frac{L_m^*}{L_m}\sim\frac{a}{4U}l^{m+1}\qquad(m=1,2);\tag{30}$$

then note that the quantities to be compared are $2\cos\omega t(a/U)E_{\theta r\theta}$ and $F_{rzr}\mathrm{e}^{i\omega t}$ (see definition of the E's on p. 4), and use the asymptotic expansions ($l\to\infty$; $z\to\infty$):

$$\left.\begin{aligned}&P_l^m(\cos\theta)\sim(-1)^m\sqrt{[2/\pi l\sin\theta]}\,l^m\cos\left[\left(l+\frac{1}{2}\right)\theta+m\frac{\pi}{2}-\frac{\pi}{4}\right]\\&H_m^{(2)}(z)\sim\sqrt{[2/\pi z]}\exp\left[-i\left(z-m\frac{\pi}{2}-\frac{\pi}{4}\right)\right]\end{aligned}\right\}\tag{31}$$

to obtain equivalence between the two spectral contributions. This result can readily be extended to the other coefficients; the six F's which are identically zero in formulae (25) correspond to coefficients E_{ijk} increasing slower than $(L_1/r_s)l^{5/2}$ or $(L_2/r_s)l^{7/2}$ in formulae (15), since it is well-known that $L_1/L_2=O(l)$ as $l\to\infty$.

In the case of spheroidal modes and Rayleigh waves, one would proceed in a similar way, after noticing that the normalization assumption of identical y_1's at the surface will imply

$$y_j\text{ (spheroidal mode)}/y_j\text{ (Rayleigh wave)}\to 1\ (j=1,2)\text{ but }\sim\frac{1}{l}\ (j=3,4)\,,\tag{32}$$

so that:

$$\frac{K_j^*}{K_j}\sim\frac{a}{4U}l^j\quad(j=1,2)\qquad\text{and}\qquad\frac{K_j^*}{K_j}\sim\frac{a}{4U}l^{j-3}\quad(j=3,4)\tag{33}$$

(where we have defined $K_3=K_4(y_2r_s/\mu y_1)$). Here again, we must pay attention to the fact that as $l\to\infty$, only principal terms in the E's and F's will be equivalent, and to the following rules: $K_2/K_1=O(1/l)$; $K_4/K_3=O(1/l)$.

4.2 Asymptotic equivalence with directivity formalism

Anticipating somewhat over the results of Sec. 5.1, and again drawing on an example, we will now use our Rayleigh wave results (29) to investigate unidirectional horizontal rupture (at velocity v_r) in the case of a strike-slip fault of length A. The only non-zero terms in the tensors M_{ij} and M_{ijk} are:

$$\left.\begin{aligned} M(t)=M_{r\phi}(t)=M_{\phi r}(t)&=\begin{cases} 0 & (t<0) \\ -Mv_r t/\Lambda & (0\le t\le \Lambda/v_r) \\ -M & (t>\Lambda/v_r) \end{cases} \\ R(t)=M_{rr\phi}(t)=M_{r\phi r}(t)=\frac{1}{2}M_{\phi rr}(t)&=\begin{cases} 0 \\ -(M\Lambda/2)(v_r t/\Lambda)^2 \\ -(M\Lambda/2) \end{cases} \quad \begin{matrix} \text{in the} \\ \text{same} \\ \text{intervals,} \end{matrix} \end{aligned}\right\} \tag{34}$$

where M is the total (static) seismic moment released. At first order in the variable $(\omega\Lambda/v_r)$, this leads to:

$$\dot{M}(\omega)=M(1-i\omega\Lambda/2v_r) \qquad \text{and} \qquad \dot{R}(\omega)=\frac{M\Lambda}{2}(1-2i\omega\Lambda/3v_r)\,.$$

Combining both orders $n=1$ and $n=2$, and keeping only terms of order $(\omega\Lambda/v_r)$, one finds that the spectral amplitude excited by this system,

$$-(D_{r\phi}+D_{\phi r})\dot{M}(\omega)-\frac{1}{2}(F_{rr\phi}+F_{r\phi r}+2F_{\phi rr})\dot{R}(\omega)\,,$$

is equivalent to

$$MK_2{}^*Q_2 \sin 2\phi\left[1-\frac{i\omega\Lambda}{2}\left(\frac{1}{v_r}-\frac{\cos\phi}{C}\right)\right], \tag{35}$$

an expression identical to the first-order expansion of the directivity formula (BEN-MENAHEM, 1961):

$$MK_2{}^*Q_2 \sin 2\phi \exp\left[-\frac{i\omega\Lambda}{2}\left(\frac{1}{v_r}-\frac{\cos\phi}{C}\right)\right]\mathrm{sinc}\left[\frac{\omega\Lambda}{2}\left(\frac{1}{v_r}-\frac{\cos\phi}{C}\right)\right]. \tag{36}$$

In reaching this result, we have simply assumed that kr is large enough that $Q_3/Q_2\sim -i$ and $Q_1/Q_2\sim i$.

These results, which can easily be extended to other cases of horizontal rupture merely constitute a verification of the formalism which we have developed, in an asymptotic situation for which the higher moment method is not powerful. Formula (35) actually shows that at first order in $\omega\Lambda/v_r$, the amplitude of the wave is unchanged, and any significant analysis should be carried at least to the next order, which would involve computation of fourth-order tensors. Although this is a clear drawback of this method, we must emphasize that certain simple ruptures, such as those containing a strong vertical component, which may affect the value of the local excitation, cannot be handled by simple directivity theory. As we will see in Sec. 5, higher monent theory can provide important results even under the restriction of using only terms corresponding to $n=2$.

4.3 The "hybridization" paradox

Two of the most fundamental geometries for point source double-couples are strike-slip and dip-slip on a vertical fault. It is well known that they give

rise to simple radiation patterns for body waves and surface waves, in the latter case independently from frequency and source depth. In the case of normal modes, they are the basic mechanisms characteristic of the coefficients L_1, K_1 (dip-slip) and L_2, K_2 (strike-slip). No coupling between the two-lobe and four-lobe radiation patterns exists for these pure geometries.

It may therefore appear puzzling why, in an excitation coefficient such as $E_{\phi\theta\theta}$, which is involved in the horizontal propagation of a strike-slip fault, one should find the coefficient L_1, characteristic of dip-slip geometry (or the combination $[K_0-K_1]$ in the spheroidal case). This brings up the following paradox: Let us position ourselves at a depth such that the strike-slip coefficient L_2 vanishes (with $y_1(r)$, for example at the crossover point of an overtone eigenfunction). A strike-slip source at that depth should not excite the particular mode involved, but a strike-slip propagating horizontally would! The answer to the paradox resides in the sphericity of the Earth: the moments M_{ijk} are computed in a Cartesian frame; if we assume that the direction of slip is constant in space, the source will grow a small dip-slip component as we travel away from the reference point $\hat{\boldsymbol{\xi}}=\mathbf{0}$ at a constant depth, and the mode frame rotates with the local vertical. A similar situation arises for spheroidal modes, but in the case of surface waves, as the radius of the Earth goes to infinity, strike-slip and dip-slip coefficients corresponding to horizontal rupture remain decoupled, as documented by formulae (25) and (29).

One could then discuss whether the use of the present formalism is legitimate in the case of normal modes, when sphericity is implied, and horizontal propagation is actually not linear propagation. However, one must put this discussion in perspective: even for the longest known seismic ruptures (e.g., Chile, 1960: 850 km), the deviation of the local vertical is less than 10 degrees; for most large events, the figure is closer to 2 or 3 degrees (see for example GELLER, 1976). It would be futile to address the problem of whether the slip vector remains parallel to itself, or rotates with the local vertical along the fault, when one realizes that slip angles for large events are usually determined to a precision no better than ± 5 degrees, even with the help of sophisticated techniques (ROMANOWICZ, 1981). Conversely, this example may be used to bear in mind that heterogeneity of the slip angle in the fault plane, due for example to the presence of discontinuous asperities, will affect normal mode excitation, and consequently the resolution of moment tensor inversion.

5. *Application to Simple Cases of Finite Sources*

5.1 Radial and transverse integrals

From the general definition of M_{ijk}, it is clear that $M_{ijk}=M_{ikj}$, and therefore, one needs a priori compute 18 independent components of the third-order tensor M. We will show, however, that under extremely general conditions on the faulting, only two independent functions need be computed. We will assume that

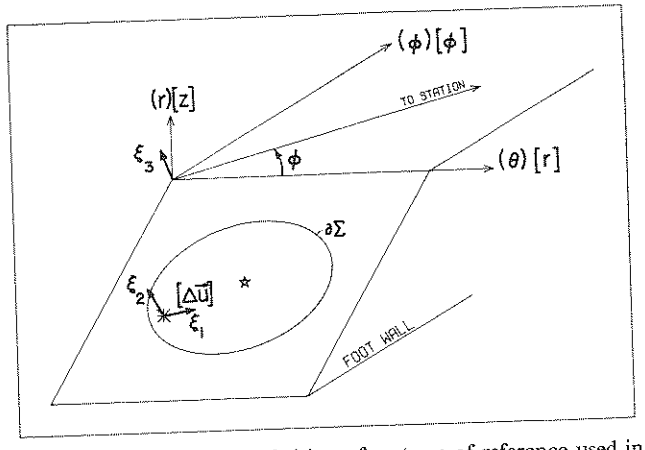

Fig. 1. Geometry of faulting and definition of systems of reference used in this study. The displacement vector is that of the hanging wall (not shown) relative to the foot wall. The frame used in the normal mode study is shown in parentheses, that used with surface waves in brackets. $\partial\Sigma$ represents the boundary of the rupture area. The asterisk represents the hypocenter, where the rupture initiates; the star represents the static centroid (assuming that $[\Delta u]$ is independent of ξ), as $\tau\rightarrow\infty$.

a. The rupture propagates in the plane of faulting, and

b. The direction of slip remains constant during the faulting.

In other words, and in the geometry of Fig. 1, these conditions merely require that the system of axes $[\hat{e}_1, \hat{e}_2, \hat{e}_3]$ remain fixed during the rupture. However, the nature of the rupture (unidirectional, circular, etc. . . .), as well as the shape of the faulting area (more generally speaking the function $[\Delta u(\xi, \tau)]$) are subject to no conditions. These restrictions apply to a very large number of earthquake sources. Furthermore, in some instances when they do not apply, they can still be applied by parts to individual sections of the faulting (that is the case, for example, for the Izu-Oshima earthquake of 1978 (SHIMAZAKI and SOMMERVILLE, 1979), which featured a bend along the fault trace).

Then, it is immediate to show from Eq. (2), that at order $n=1$ the only non-zero components of M_{ij} are

$$M_{13}(\tau)=M_{31}(\tau)=\int_{\Sigma}\mu(\xi)[\Delta u(\xi,\tau)]\mathrm{d}\xi_1\mathrm{d}\xi_2\,. \tag{37}$$

Similarly, at order $n=2$, and after a few integrations by parts, making use of the finiteness of the source, one finds:

$$\left.\begin{aligned} M_{113}(\tau)=M_{131}(\tau)=\frac{1}{2}M_{311}(\tau)&=\int_{\Sigma}\mu(\xi)\xi_1[\Delta u(\xi,\tau)]\mathrm{d}\xi_1\mathrm{d}\xi_2=R(\tau)\\ M_{123}(\tau)=M_{132}(\tau)=M_{312}(\tau)=M_{321}(\tau)&=\int_{\Sigma}\mu(\xi)\xi_2[\Delta u(\xi,\tau)]\mathrm{d}\xi_1\mathrm{d}\xi_2=T(\tau)\end{aligned}\right\} \tag{38}$$

all other $M_{ijk}=0$,

so that all components of the tensor M_{ijk} can be computed from the two independent functions $R(\tau)$ and $T(\tau)$, representing the moment of the seismic slip released at time τ in the directions parallel and perpendicular to the slip. We shall call these functions the radial and transverse integrals. Their computation is straightforward (and inexpensive) given any source model, however complex its geometry and slip history may be. It is then possible to rotate the $E_{\alpha\beta\gamma}$'s from the $(\hat{r}, \hat{\theta}, \hat{\phi})$ frame of the mode to the $(\hat{e}_1, \hat{e}_2, \hat{e}_3)$ frame of the source, so that the $n=2$ term of Eq. (5):

$$\frac{1}{2} E_{\alpha\beta\gamma} \dot{M}_{\alpha\beta\gamma}(\tau) \qquad (27 \text{ terms})$$

merely becomes: $(1/2)[ER\ \dot{R}(\tau)+ET\ \dot{T}(\tau)]$ (2 independent terms). The rotation from the $E_{\alpha\beta\gamma}$'s to ER and ET involves only the direction cosines $a_{i\alpha}$ between the two frames, and is immediate on a computer:

$$\left.\begin{aligned} ER &= E_{\alpha\beta\gamma}(a_{1\alpha}a_{1\beta}a_{3\gamma}+a_{1\alpha}a_{1\gamma}a_{3\beta}+2a_{3\alpha}a_{1\beta}a_{1\gamma}) \\ ET &= E_{\alpha\beta\gamma}(a_{1\alpha}a_{2\beta}a_{3\gamma}+a_{1\alpha}a_{3\beta}a_{2\gamma}+a_{3\alpha}a_{1\beta}a_{2\gamma}+a_{3\alpha}a_{2\beta}a_{1\gamma})\,. \end{aligned}\right\} \qquad (39)$$

The coefficients $a_{i\alpha}$ are readily computed from the geometry shown on Fig. 1.

5.2 Application to a few simple geometries

In order to study a few simple cases, we will consider a set of two focal mechanisms, and two rupture geometries: strike-slip and dip-slip events on a vertical fault, with the propagation of the rupture along a rectangular fault zone, whose main dimension will be either horizontal or vertical (see Fig. 2). The reference source (and starting point of the rupture) will be placed at the center of the small dimension of the fault rectangle, so that by symmetry, either $R(t)$ or $T(t)$ will vanish identically.

For each of the geometries involved, we use four sources of different moments (see Table 1), with a common geometric scaling, and a constant rupture velocity of 3 km/sec; this introduces similar scaling in time, which affects excitation by

Table 1. Parameters of the two models of rupture used in Sec. 5, for the 4 scales of sources involved (see Fig. 2).

Nature of rupture	Moment (dyn/cm)	Δu (cm)	Hypocentral depth (km)	Horizontal extent of rupture from hypocenter (km)	Vertical extent of rupture from hypocenter (km)	Static centroid depth (km)	Rupture velocity (km/sec)
Horizontal	10^{28}	175	20	0,200	−20, 20	20	3
Horizontal	10^{27}	76	20	0,93	−9.3, 9.3	20	3
Horizontal	10^{26}	40	20	0,43	−4.3, 4.3	20	3
Horizontal	10^{25}	17.5	20	0,20	−2, 2	20	3
Vertical	10^{28}	186	20	−25, 25	−130, 20	75	3
Vertical	10^{27}	91	20	−12, 12	−60, 9.3	51	3
Vertical	10^{26}	44	20	−5.4, 5.4	−28, 4.3	32	3
Vertical	10^{25}	18.6	20	−2.5, 2.5	−13, 2	25.5	3

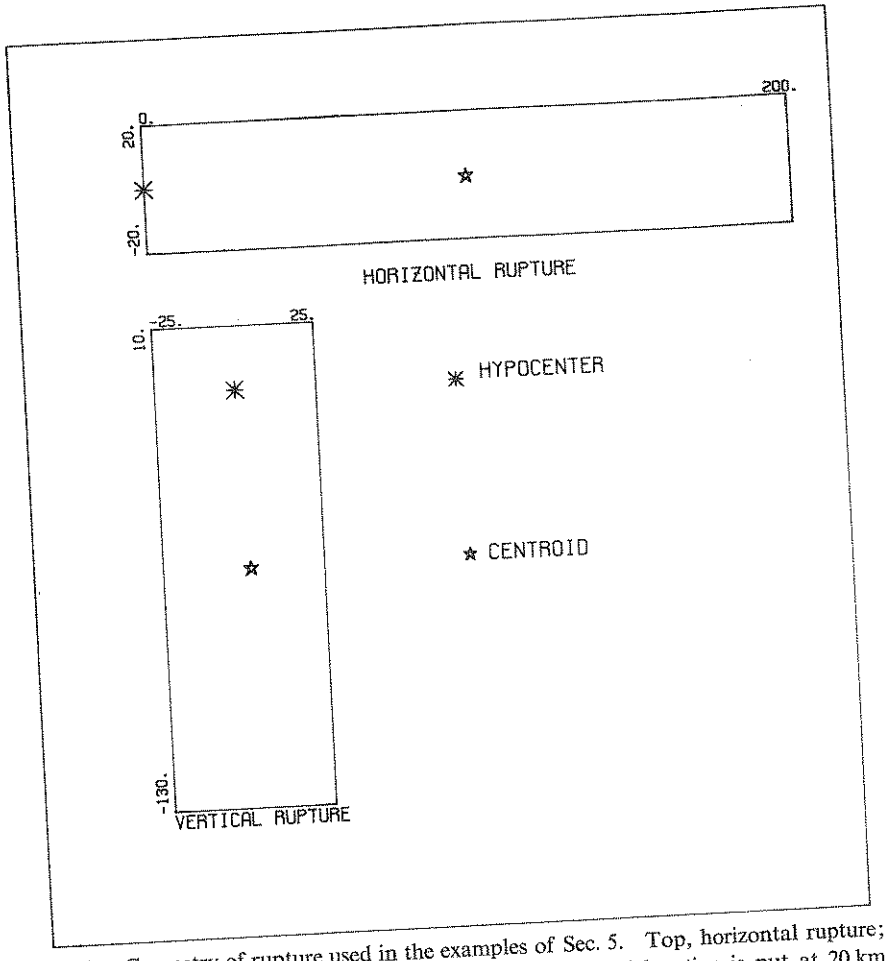

Fig. 2. Geometry of rupture used in the examples of Sec. 5. Top, horizontal rupture; bottom, vertical rupture. In all cases, the hypocentral location is put at 20 km depth (asterisk); in the case of the 10^{28} dyn/cm source, the dimensions of the source are given in km, in a horizontal-vertical frame centered at the hypocenter. For the other values of the moments, the units must be scaled. The star depicts the position of the static centroid (assuming again that the final displacement is homogeneous along the fault). In all cases, there remains a choice of dip-slip or strike-slip focal mechanism.

second-order moments through the term $\dot{M}_{ij}(\omega)$.

In the case of strike-slip on a vertical fault, the system $(\hat{e}_1, \hat{e}_2, \hat{e}_3)$ corresponds to $(\hat{\theta}, \hat{r}, -\hat{\phi})$, so that the only non-zero components of M_{ijk} are:

$$\left.\begin{aligned} M_{\theta\theta\phi} = M_{\theta\phi\theta} = \frac{1}{2} M_{\phi\theta\theta} = -R(t) \qquad & \text{(horizontal rupture), or} \\ M_{\theta r\phi} = M_{\theta\phi r} = M_{\phi r\theta} = M_{\phi\theta r} = -T(t) \qquad & \text{(vertical rupture).} \end{aligned}\right\} \tag{40}$$

Similarly, in the case of a dip-slip on a vertical fault, $(\hat{e}_1, \hat{e}_2, \hat{e}_3) = (\hat{r}, -\hat{\theta}, -\hat{\phi})$,

so that we will only have:

$$\left.\begin{aligned} M_{rr\phi} = M_{r\phi r} = \frac{1}{2} M_{\phi rr} = -R(t) \qquad & \text{(vertical rupture), or} \\ M_{r\theta\phi} = M_{r\phi\theta} = M_{\phi r\theta} = M_{\phi\theta r} = T(t) \qquad & \text{(horizontal rupture).} \end{aligned}\right\} \tag{41}$$

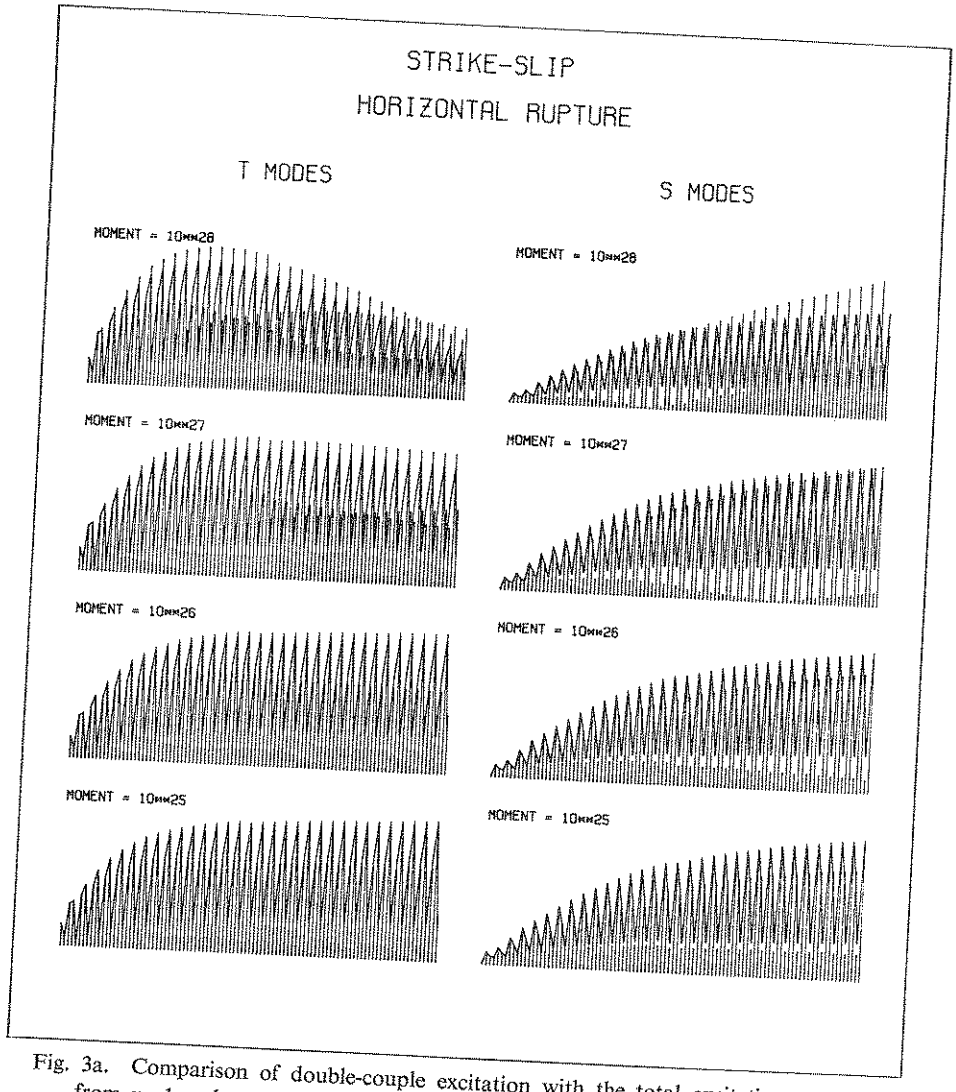

Fig. 3a. Comparison of double-couple excitation with the total excitation resulting from $n=1$ and $n=2$ terms, in the case of horizontal rupture and strike-slip focal mechanism. Left, toroidal modes; right, spheroidal modes. For each of the 4 values of the moment used, the continuous line represents the double-couple excitation, and the bars include the third-order term. In all cases, the abscissa is angular order number (l), ranging from 2 (left) to 100 (right). The vertical scale on each frame is arbitrary.

Figure 3 compares the excitation of the first fundamental toroidal and spheroidal modes ($l \leq 100$) for the double-couple point source ($n=1$) and for the combination of the $n=1$ and $n=2$ terms, for the various geometries and moments studied. On each diagram, the solid line represents the $n=1$ term (drawn continuously between individual modes to enhance legibility), and the vertical bars are relative to the combination of the second- and third-order tensors M_{ij} and M_{ijk}. The influence of the higher-order moment is described by the misfit between the top of the bars and the solid line. Generally speaking, this misfit increases with the seismic moment of the source, everything else being constant. This is expected, since the size of the rupture zone also increases, and so do the integrals

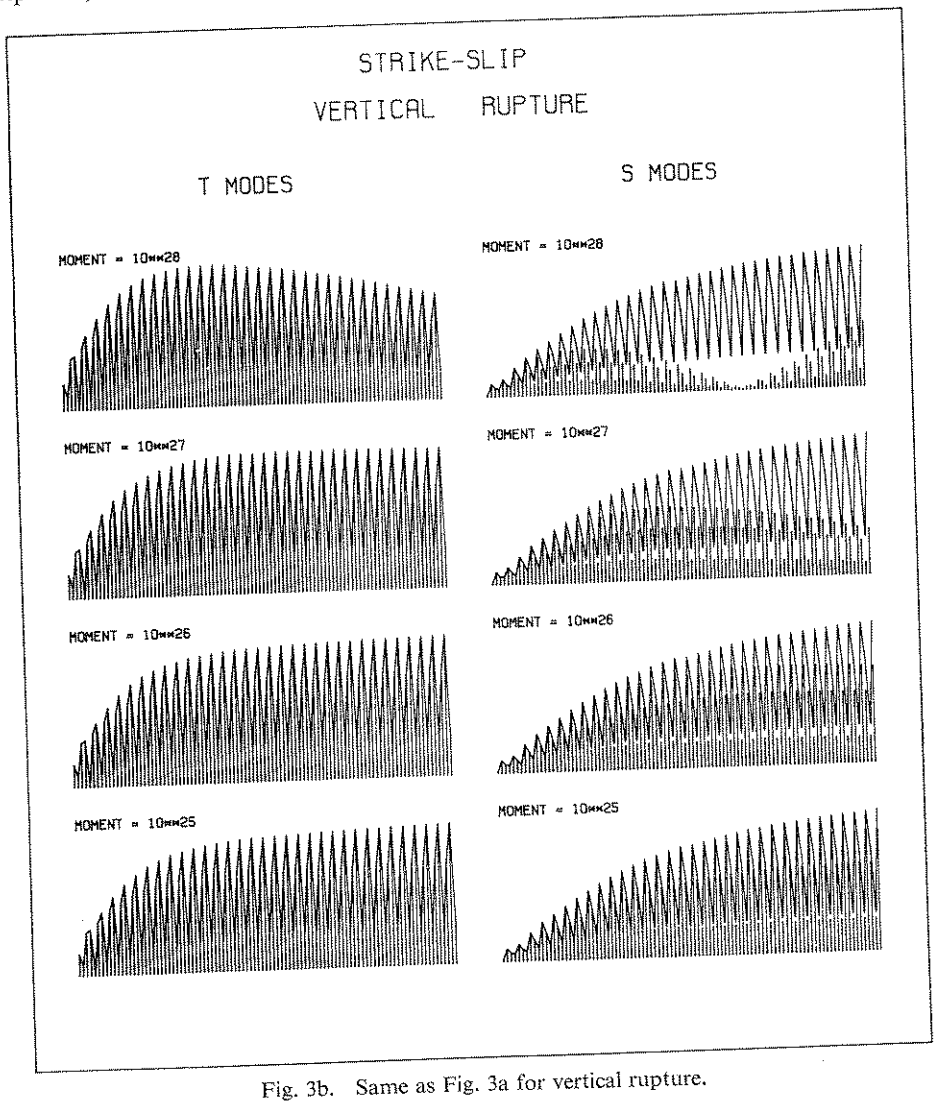

Fig. 3b. Same as Fig. 3a for vertical rupture.

$R(t)$ or $T(t)$, relative to the double-couple $M(t)$. However, a number of more subtle features warrant further discussion.

Strike-slip: In the case of a vertical rupture, the higher-mode excitation is proportional to the combination $(E_{\theta r\phi}+E_{\phi r\theta})$. In the case of toroidal modes, this equals $-(L_1/2r_s)\cos 2\phi Q_2$, a term negligible with respect to the double-couple term involving $L_2\cos 2\phi Q_2$, since at given l, and for a shallow source, $L_1 \ll L_2$. (We must make the distinction with the situation in Sec. 4.1, which involved $l\to\infty$ at a given depth, in which case $L_1/L_2=O(l)$.) For spheroidal modes, however, the $n=2$ term becomes $(K_4-K_1)(P_l^2/4r_s)\sin 2\phi$, in which $K_1\to 0$ at the surface, but K_4 does not. Consequently, we predict a different behavior for

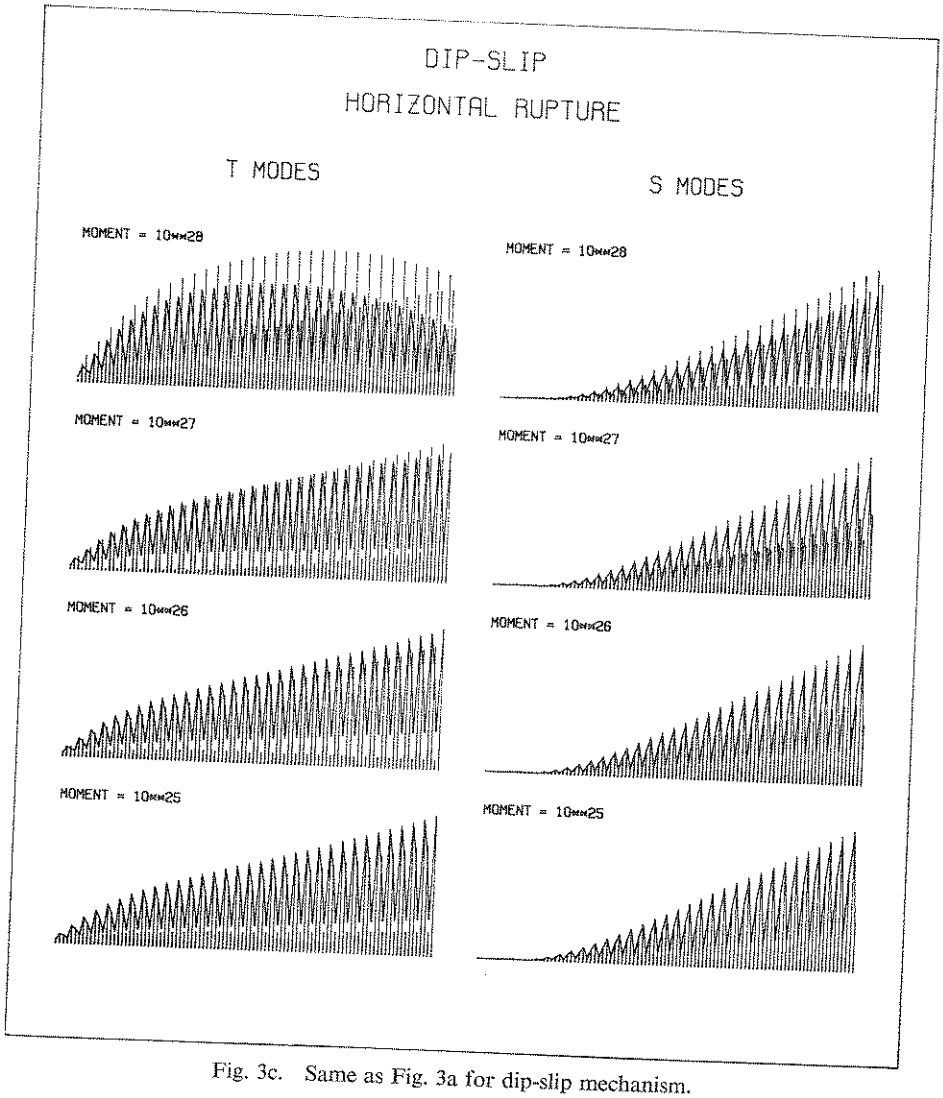

Fig. 3c. Same as Fig. 3a for dip-slip mechanism.

toroidal and spheroidal modes, clearly observed on Fig. 3a: the S modes are sensitive to the higher moment, and therefore to the size of the source, while the T modes are not. However, in the case of a horizontal rupture (Fig. 3b), the $n=2$ excitation, proportional to $[E_{\theta\theta\phi}+2E_{\phi\theta\theta}]$, leads to terms involving the same coefficients L_2 and K_2 as for the double-couple, and therefore results in substantial response to the higher-order moments, for both T and S modes.

Dip-slip: The case of the dip-slip source is of particular interest, since for shallow point sources, the double-couple excitation is very small ($K_1=L_1=0$ for $r_s=a$). For a horizontal rupture, the governing terms are now $[E_{r\theta\phi}+E_{\phi\theta r}]$, which for a torsional mode is

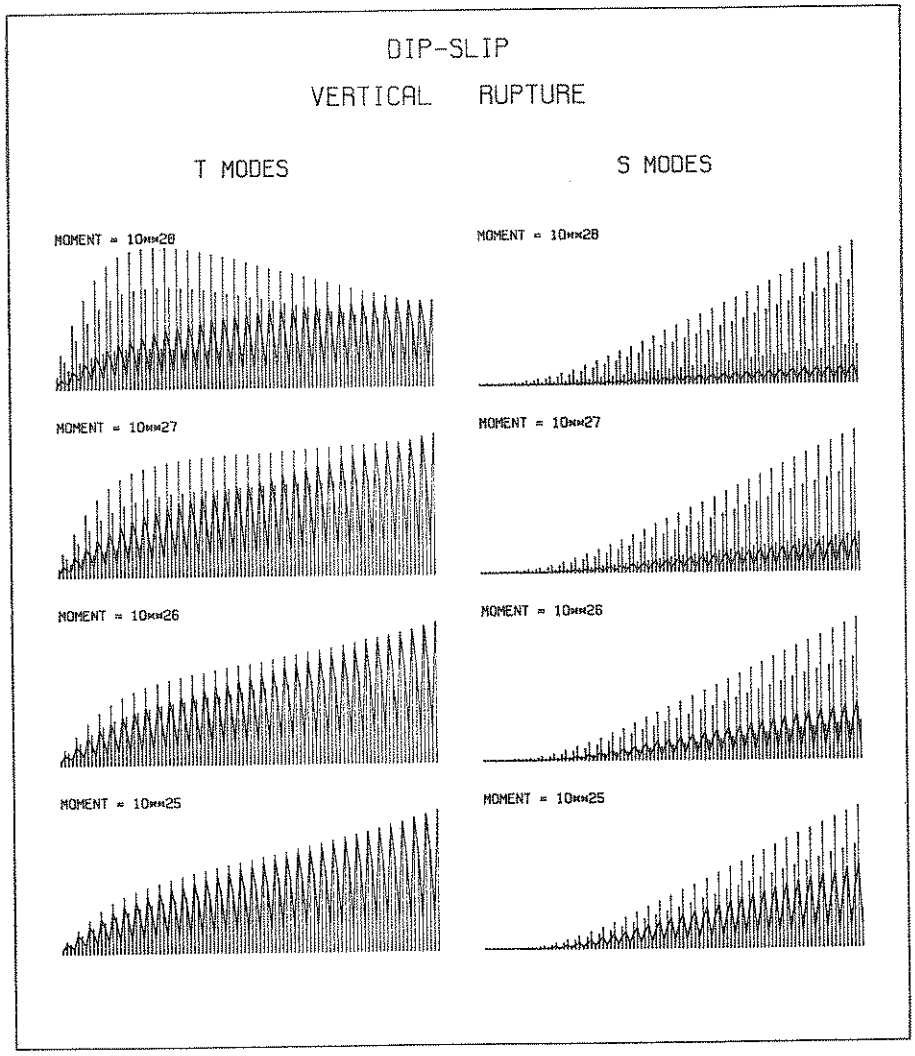

Fig. 3d. Same as Fig. 3b for dip-slip mechanism.

$$(L_2/r_s)\cos 2\phi Q_2+(L_1/r_s)(L^2Q_0-\cos 2\phi Q_2)\,. \tag{42}$$

Since $L_1 \ll L_2$, this term is on the order of L_2Q_2/r_s, as compared to L_1Q_1 for the double-couple. As seen on Fig. 3c, this results in substantial excitation by the higher moment. Similarly, for spheroidal modes, we find a term on the order of $K_2(P_l^2/4r_s)$. In the case of a vertical rupture, however, the excitation, governed by $[E_{rr\phi}+E_{\phi rr}]$, will be proportional to

$$(3L_1/r_s)Q_1\cos\phi+(L_2/r_s)Q_1\cos\phi[L^2(C^2/\beta^2-1)+2]$$

for toroidal modes. The dominant term, $(L_2/r_s)L^2Q_1(C^2/\beta^2-1)$ is roughly l times larger than its counterpart for horizontal rupture, and therefore, the higher moment contribution is very large, particularly in view of the small double-couple excitation. Similarly, for spheroidal modes, the governing term is

$$\frac{P_l^1}{r_s}\sin\phi\left[3K_1+K_5+\frac{\lambda+\mu}{\lambda+2\mu}K_3+\frac{4(\lambda+\mu)}{\lambda+2\mu}K_4+\left(\frac{\lambda}{\lambda+2\mu}-\frac{C^2}{\beta^2}\right)L^2K_2\right]. \tag{43}$$

The terms K_1 and K_3 are small for shallow sources, but the other terms are large, and again roughly l times their counterparts for horizontal rupture, giving the higher moment a strong contribution. This behavior is clearly shown on Fig. 3d.

As we will discuss in Sec. 6, the importance of the higher order term for a vertically propagating dip-slip is not unexpected, since it is geared to the rapid variation of the dip-slip excitation with depth, which vanishes at the surface, and whose depth derivative is finite, while the strike-slip coefficient for T modes has a value stationary with depth at the surface.

6. *Discussion and Perspective*

The formalism of higher moments, for which we have obtained excitation coefficients at order $n=2$ must be put into perspective and discussed, especially in view of the other techniques available (e.g., directivity) for the study of finite sources, and of the extensive algebra involved in deriving excitation coefficients.

6.1 The need for higher-order terms

As pointed out by BACKUS and MULCAHY (1976), the convergence of the series involved in the Taylor expansion of the Green's function is not fast, and may be as slow as that of $(6\pi\Lambda/\lambda)^n/n!$, where Λ is the dimension of the source, and λ the wavelength of interest, although in simple geometries, for which many components of the higher moments vanish because of symmetry, the convergence may be somewhat faster. Therefore, in order to be readily applied the present formalism should be extended to higher orders n. This does not involve any mathematical difficulty, and the differential systems satisfied by the eigenfunctions ensure that the set of excitation coefficients routinely computed for $n=1$ is sufficient to compute all coefficients at all orders n. However, the volume of algebra involved grows rapidly with n, and becomes somewhat prohibitive. It may be useful to

give a quantitative estimate of the range of constraints imposed by truncation of the series after $n=2$. Under BACKUS and MULCAHY's (1976) conservative estimate, and assuming an acceptable error of 10% from terms neglected, we must restrict ourselves to $A/\lambda \lesssim 0.05$ if we keep only $n=2$ terms, and 0.07 for $n=3$. This would correspond to dimensions of $A \lesssim 50$ km at 200 sec.

6.2 Could we do without $n=2$ terms?

It is a general property of moment theory that a change of the reference point about which the moments are computed, say from $\boldsymbol{x}_s$ to $\boldsymbol{X}_s=\boldsymbol{x}_s+\boldsymbol{\Xi}$, results in new moment components M_{IJK}, which at order $n=2$ can be written:

$$M_{IJK}=M_{ijk}+\Xi_j M_{ik}+\Xi_k M_{ij} \,. \tag{44}$$

Here, we have used the fact that the resultant of the system of forces $\boldsymbol{f}$ vanishes. One may wonder if it is possible to find a vector $\boldsymbol{\Xi}$ which will make the M_{IJK}'s vanish. In general, this is impossible, since the problem is overdetermined, but it is easy to show that under the two simplifying assumptions described in Sec. 5, the system

$$\left.\begin{aligned} \Xi_1 &= -R(\tau)\Big/\int \mu A u(\boldsymbol{\xi}, \tau)\mathrm{d}\xi_1\mathrm{d}\xi_2 \\ \Xi_2 &= -T(\tau)\Big/\int \mu A u(\xi, \tau)\mathrm{d}\xi_1\mathrm{d}\xi_2 \\ \Xi_3 &= 0 \end{aligned}\right\} \tag{45}$$

is a solution. Thus, it appears that it is possible to avoid using $n=2$ terms, provided an adequate reference point is computed. Of course, the second-order excitation coefficients at this new reference point will be slightly different from those at $\boldsymbol{x}_s$, this difference only expressing the close relationship between the E_{ijk}'s and the derivatives of the second-order coefficients.

This approach has been used in second-order moment tensor inversion by DZIEWONSKI and WOODHOUSE (1981), who call the point $\boldsymbol{X}_s$ the centroid of the hypocenter, which can significantly deviate from the location of the earthquake, as computed from first motion data. However, it is clear from Eq. (45) that the vector $\boldsymbol{\Xi}$, and therefore the centroid, is time-dependent. It would of course be possible to define a centroid at each time τ, or better at each frequency ω. But this would lead to a readjustment of the parameter $\boldsymbol{\xi}$ in the Green's function (and therefore to its entire recomputation) everytime the centroid is moved, that is at each frequency, or for each normal mode. This procedure is precisely of the type involved in Eq. (1) which has been avoided, whenever possible both through the centroid theory, or the present approach.

We have investigated whether the third-order terms would play a significant role at the frequencies of normal mode excitation, once computed in the frame of the static centroid $\boldsymbol{\Xi}_\infty$ [$\tau \to \infty$ in Eq. (45)], in the case of a vertical rupture along a dip-slip fault, and for toroidal modes. In this geometry, and for each of

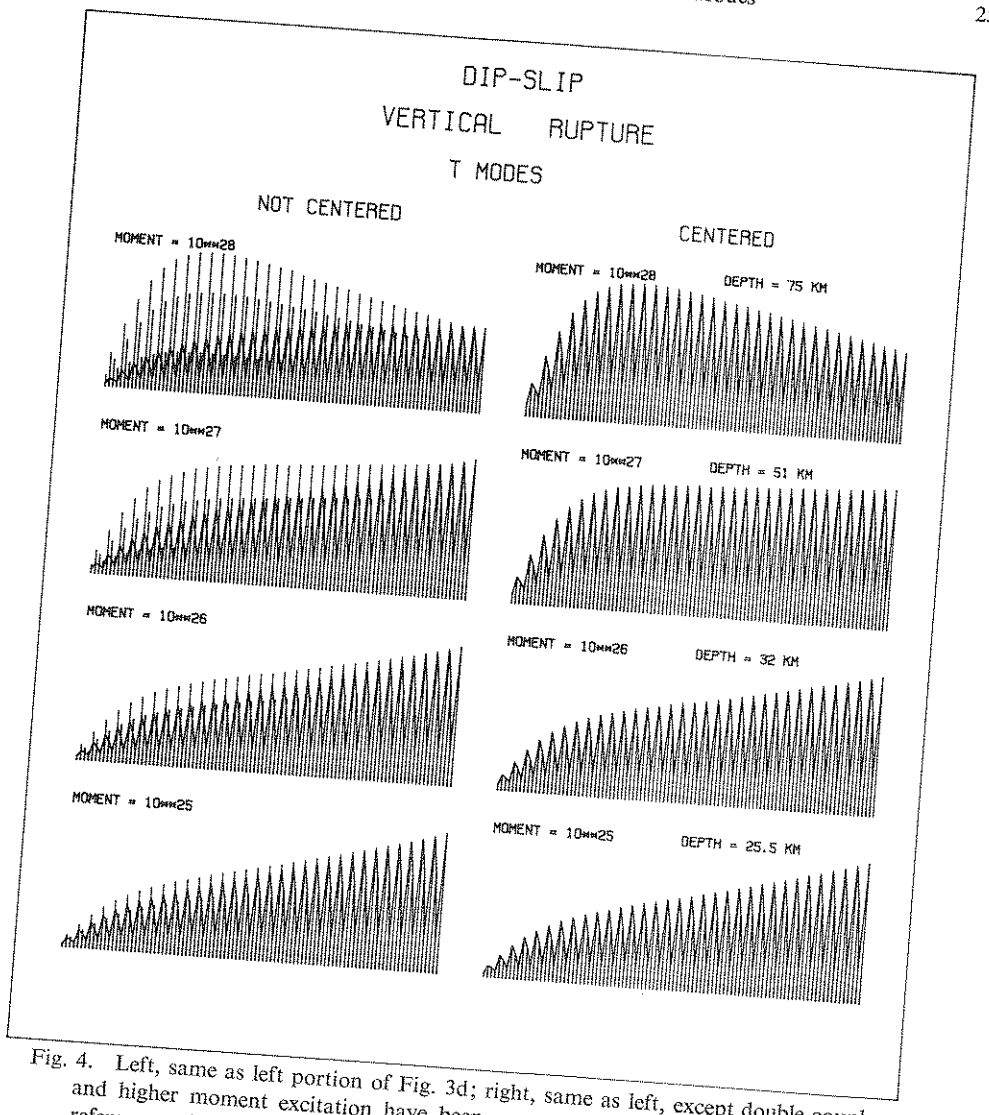

Fig. 4. Left, same as left portion of Fig. 3d; right, same as left, except double-couple and higher moment excitation have been computed using the static centroid as reference point (with depth depending on size of event).

the four scaled ruptures used in Sec. 5, we have computed the depth of the static centroid and calculated the excitation by the second- and third-order moments using the centroid as reference point $\bar{\boldsymbol{\xi}}=\mathbf{0}$. Results are shown on the right side of Fig. 4, and compared to those from Fig. 3d (with the reference point at the location of initiation of the rupture) on the left. It is found that, in the frame of the centroid, second-order coefficients are sufficient to adequately describe the total excitation, down to periods on the order of 100 sec. This result was to be expected, since the simple mode of rupture involved in this particular example

is relatively short-lived (the total rupture lasting only 45 sec, in the case of the largest source). However, in the case of a slower rupture mechanism, such as that involved for a foreshock and a main shock sequence, the centroid would be significantly time-dependent in the range of frequencies of normal mode excitation, and the third-order terms would contribute significantly.

Additionally, the calculation of the static centroid Ξ_∞ in the forward problem requires knowledge of the integrals R and T, and the F_{ijk}'s are necessary for any perturbation scheme, or inversion process automating its search. Finally, as pointed out by DZIEWONSKI and WOODHOUSE (1981), the centroid model is not applicable to ruptures of a more complex nature.

6.3 Importance of source size on excitation

Perhaps the most important result of the present study is the size of the contribution of third-order moments to the excitation: substantial excitation of the Earth's modes by third-order moments can take place even for relatively small earthquake sources. The examples studied in Sec. 5 have shown that events in the moment range 10^{25}–10^{26} dyn/cm ($M_s \simeq 6$) with fault dimensions on the order of 20 to 30 km can give rise, for dip-slip geometry, to significant $n=2$ terms, at periods on the order of 100 sec, despite the fact that such earthquakes are usually considered to be adequately represented by point source double-couples. We have shown that, even for such small events, an important contribution to the excitation is made by vertical ruptures for shallow dip-slip mechanisms although double-couple theory predicts weak excitation. Conversely, in the case of strike-slip mechanisms, the vertical rupture contributes no significant excitation. Vertical rupture will therefore affect significantly the relative excitation of dip-slip and strike-slip components of an earthquake. This property is of course an expression of the well-known singularity of the dip-slip excitation for shallow sources, which leads to instability in moment tensor inversion (KANAMORI and GIVEN, 1980), and to a critical influence of depth on its results. Although techniques have been developed recently, which permit determination of the centroid depth simultaneously with moment tensor inversion (ROMANOWICZ, 1981), their precision is about 5 km, which unfortunately, is also comparable to the offset from the original epicenter to the centroid in our example of smallest moment. In other words, these techniques might not, in the case of $M_s=6$ events, distinguish between the original reference point and the static centroid, leaving third-order terms of significant importance, which will in turn bias the geometry of the inverted moment tensor.

Furthermore, it has generally been observed that, although the normal mode frequencies observed on earthquake spectra (e.g., on records of the IDA network) are in excellent agreement with theoretical computations, their amplitudes are often grossly misfit. JORDAN and SILVER (1981) have suggested that structural lateral heterogeneity in the Earth could affect excitation coefficients by as much as 30%. Notwithstanding this very possible source of misfit between classically computed

and observed amplitudes of normal mode spectra, we think that source finiteness can contribute a considerable amount to normal mode excitation, in particular through the influence of depth and of slight variations in the geometry of the faulting, parameters which are not readily incorporated in methods such as directivity widely used to account for this phenomenon. Source dimensions should be taken into account in such studies, either through the centroid approach (when applicable), or through the systematic use of higher moments, of which this paper presents the formalism at order $n=2$.

6.4 Potential application to tsunami excitation

Finally, the present formalism and its extension to higher orders could be applied easily to tsunami generation, a particular case of spheroidal mode theory, for a gravitating Earth, with an oceanic layer (WARD, 1980). Because of their low phase velocity, tsunami modes have small wavelengths, and directivity effects of a tremendous amplitude and devastating character are predicted and observed (SPAETH and BERKMAN, 1969; BEN-MENAHEM and ROSENMAN, 1972). Also, because of the poor penetration of tsunami eigenfunctions into the solid Earth, tsunami excitation is critically dependent upon source depth (WARD, 1980), and vertical rupture will contribute significantly to the excitation.

All the formalism described in Sec. 2 can be applied to tsunami excitation, but we should be careful to include the gravitational components (y_5, y_6) to the eigenvector, in order to obtain correct expressions for the excitation coefficients. It is straightforward to show that only the second derivatives of the displacement eigenfunctions y_1 and y_3 are affected by the gravity terms, so that the expressions for the A_{ij}'s and most of the E_{ijk}'s are unchanged. Only E_{rrr}, $E_{\theta rr}$, and $E_{\phi rr}$ must be corrected by adding the following terms to the expressions given in formulae (18):

$$\left.\begin{aligned} {}^6E_{rrr} &= \frac{1}{2}\frac{gr}{\alpha^2}[4K_4 - L^2K_2 + K_7]\frac{P_l^0}{r} \\ {}^6E_{\theta rr} &= -\frac{1}{2}\frac{gr}{\beta^2}[K_4 - K_8]\frac{P_l^1}{r}\cos\phi \\ {}^6E_{\phi rr} &= -\frac{1}{2}\frac{gr}{\beta^2}[K_4 - K_8]\frac{P_l^1}{r}\sin\phi\,, \end{aligned}\right\} \tag{46}$$

where we have defined:

$$\left.\begin{aligned} K_7 &= K_4\frac{r}{g}\frac{y_6}{y_1} \\ K_8 &= K_4\frac{1}{g}\frac{y_5}{y_1} \end{aligned}\right\} \tag{47}$$

and g is the local acceleration of gravity at $r=r_s$.

The higher moment formalism may be of great interest to study tsunami generation in complex cases, such as those involving vertical rupture in earthquakes

of the Sanriku type, breaking the lithosphere away from the subduction area (KANAMORI, 1972), or the Kurile Islands earthquakes of 1975, for which rupture was suggested to have taken place in relatively soft material, located in the wedge of the subduction zone (FUKAO, 1979). In this latter case, the present theory allows to easily change the parameters of the rupture, in particular the rigidity $\mu(\xi)$ along the fault, and could be a very powerful investigative tool.

7. *Conclusion*

We have derived excitation coefficients of normal modes and surface waves for the case $n=2$, and shown on a number of examples that higher moments can play a significant role in the excitation of normal modes, especially in the case of vertical rupture. Although the algebra and book-keeping involved may prevent extension of this formalism to much higher orders, we believe that this approach will prove useful, in providing insight into the influence of source finiteness, notably in its vertical extent, and even for moderately-sized earthquakes, onto a range of phenomena including normal mode excitation, moment tensor inversion, the search for deep lateral heterogeneity, and the understanding of tsunami excitation.

I thank Hiroo Kanamori and Barbara Romanowicz for preprints of their papers. Lane Johnson kindly sent a copy of Brian Stump's Thesis. This research was supported by the National Science Foundation, under Grants EAR-79-03907 and EAR-81-06106.

APPENDIX

We give here for reference the expression of the first- and second-order tensor derivatives of the displacement, both in spherical and cylindrical polar coordinates. We define u as the seismic displacement, v as its first spatial derivative and w as its second spatial derivative, so that in Cartesian coordinates: $v_{ij}=u_{i,j}$ and $w_{ijk}=u_{i,jk}$. Formulae (A.3) and (A.4) should be completed by the obvious relation $w_{\alpha\beta\gamma}=w_{\alpha\gamma\beta}$.

Spherical polars:

$$\left.\begin{aligned} v_{rr} &= u_{r,r} \\ v_{\theta r} &= u_{\theta,r} \\ v_{\phi r} &= u_{\phi,r} \\ v_{r\theta} &= \frac{1}{r}u_{r,\theta}-\frac{1}{r}u_{\theta} \\ v_{\theta\theta} &= \frac{1}{r}u_{\theta,\theta}+\frac{1}{r}u_{r} \\ v_{\phi\theta} &= \frac{1}{r}u_{\phi,\theta} \end{aligned}\right\} \qquad \text{(A.1)}$$

$$
\left.
\begin{aligned}
v_{r\phi} &= \frac{1}{r\sin\theta}u_{r,\phi} - \frac{1}{r}u_{\phi} \\
v_{\theta\phi} &= \frac{1}{r\sin\theta}u_{\theta,\phi} - \frac{1}{r}u_{\phi}\cot\theta \\
v_{\phi\phi} &= \frac{1}{r\sin\theta}u_{\phi,\phi} + \frac{1}{r}u_{\theta}\cot\theta + \frac{1}{r}u_{r}\,.
\end{aligned}
\right\}
$$

Cylindrical polars:

$$
\left.
\begin{aligned}
v_{rr} &= u_{r,r} \\
v_{\phi r} &= u_{\phi,r} \\
v_{zr} &= u_{z,r} \\
v_{rz} &= u_{r,z} \\
v_{\phi z} &= u_{\phi,z} \\
v_{zz} &= u_{z,z} \\
v_{r\phi} &= \frac{1}{r}[u_{r,\phi} - u_{\phi}] \\
v_{\phi\phi} &= \frac{1}{r}[u_{\phi,\phi} + u_{r}] \\
v_{z\phi} &= \frac{1}{r}u_{z,\phi}\,.
\end{aligned}
\right\} \tag{A.2}
$$

Spherical polars:

$$
\left.
\begin{aligned}
w_{rrr} &= u_{r,rr} \\
w_{rr\theta} &= \frac{1}{r}u_{r,r\theta} - \frac{1}{r}(v_{r\theta} + v_{\theta r}) \\
w_{rr\phi} &= v_{r\phi,r} \\
w_{r\theta\theta} &= \frac{1}{r}\left[\frac{1}{r}(u_{r,\theta\theta} - u_{\theta,\theta}) + v_{rr} - v_{\theta\theta}\right] \\
w_{r\theta\phi} &= \frac{1}{r}\left[\frac{1}{r\sin\theta}u_{r,\phi\theta} - \frac{1}{r\sin\theta}u_{r,\phi}\cot\theta - (v_{\phi\theta} + v_{\theta\phi})\right] \\
w_{r\phi\phi} &= \frac{1}{r\sin\theta}\left[\frac{1}{r\sin\theta}u_{r,\phi\phi} - \frac{2}{r}u_{\phi,\phi} - \frac{2}{r}u_{\theta}\cos\theta + \left(u_{r,r} - \frac{1}{r}u_{r}\right)\sin\theta \right. \\
&\qquad \left. + \frac{1}{r}u_{r,\theta}\cos\theta\right] \\
w_{\theta rr} &= u_{\theta,rr} \\
w_{\theta r\phi} &= v_{\theta\phi,r} \\
w_{\theta\theta\theta} &= \frac{1}{r}\left[\frac{1}{r}u_{\theta,\theta\theta} + \frac{2}{r}u_{r,\theta} - \frac{1}{r}u_{\theta} + u_{\theta,r}\right] \\
w_{\theta\theta\phi} &= \frac{1}{r}[v_{\theta\phi,\theta} + v_{r\phi}]
\end{aligned}
\right\} \tag{A.3}
$$

$$
\begin{aligned}
&w_{\phi rr}=u_{\phi,rr}\\
&w_{\phi r\theta}=v_{\phi\theta,r}\\
&w_{\phi r\phi}=v_{\phi\phi,r}\\
&w_{\phi\theta\theta}=\frac{1}{r}\left[\frac{1}{r}u_{\phi,\theta\theta}+u_{\phi,r}\right]\\
&w_{\phi\theta\phi}=\frac{1}{r}v_{\phi\phi,\theta}\\
&w_{\phi\phi\phi}=\frac{1}{r\sin\theta}\left[\frac{1}{r\sin\theta}u_{\phi,\phi\phi}+\frac{2}{r}u_{r,\phi}-\sin\theta u_{\phi,r}+\frac{2}{r}\cot\theta u_{\theta,\phi}\right.\\
&\qquad\left.+\frac{1}{r}\cos\theta u_{\phi,\theta}\right]\\
&w_{\theta r\theta}=v_{\theta\theta,r}\\
&w_{\theta\phi\phi}=\frac{1}{r^2\sin^2\theta}[u_{\theta,\phi\phi}-2\cos u_{\phi,\phi}]+\frac{1}{r}u_{\theta,r}+\frac{1}{r^2}[u_{\theta,\theta}\cot\theta-u_\theta\cot^2\theta]\,.
\end{aligned}
$$

Cylindrical polars:

$$
\begin{aligned}
&w_{rrr}=u_{r,rr}\\
&w_{rr\phi}=u_{r\phi,r}\\
&w_{rrz}=u_{r,rz}\\
&w_{r\phi\phi}=\frac{1}{r}\left[\frac{1}{r}(u_{r,\phi\phi}-2u_{\phi,\phi}-u_r)+u_{r,r}\right]\\
&w_{r\phi z}=\frac{1}{r}[u_{r,\phi z}-u_{\phi,z}]\\
&w_{rzz}=u_{r,zz}\\
&w_{\phi rr}=u_{\phi,rr}\\
&w_{\phi r\phi}=v_{\phi\phi,r}\\
&w_{\phi rz}=u_{\phi,rz}\\
&w_{\phi\phi\phi}=\frac{1}{r}\left[\frac{1}{r}(u_{\phi,\phi\phi}+2u_{r,\phi}-u_\phi)+u_{\phi,r}\right]\\
&w_{\phi\phi z}=v_{\phi\phi,z}\\
&w_{\phi zz}=u_{\phi,zz}\\
&w_{zrr}=u_{z,rr}\\
&w_{zr\phi}=v_{z\phi,r}\\
&w_{zrz}=u_{z,rz}\\
&w_{z\phi\phi}=\frac{1}{r}\left[\frac{1}{r}u_{z,\phi\phi}+u_{z,r}\right]\\
&w_{z\phi z}=v_{z\phi,z}\\
&w_{zzz}=u_{z,zz}\,.
\end{aligned}
\qquad\text{(A.4)}
$$

REFERENCES

AKI, K. and P. G. RICHARDS, *Quantitative Seismology*, 932 pp., W. H. Freeman, San Francisco, 1980.

BACKUS, G. and M. MULCAHY, Moment tensors and other phenomenological descriptions of seismic sources. I. Continuous displacements, *Geophys. J. R. Astron. Soc.*, **46**, 341–361, 1976.

BEN-MENAHEM, A., Radiation of seismic surface waves from finite moving sources, *Bull. Seismol. Soc. Am.*, **51**, 401–435, 1961.

BEN-MENAHEM, A. and M. ROSENMAN, Amplitude patterns of tsunami waves from submarine earthquakes, *J. Geophys. Res.*, **77**, 3097–3128, 1972.

DZIEWONSKI, A. M. and J. H. WOODHOUSE, Analysis of complex earthquakes, *EOS, Trans. Am. Geophys. Union*, **62**, 330, 1981 (abstract).

FUKAO, Y., Tsunami earthquakes and subduction processes near deep-sea trenches, *J. Geophys. Res.*, **84**, 2303–2314, 1979.

GELLER, R. J., Scaling relations for earthquake source parameters and magnitudes, *Bull. Seismol. Soc. Am.*, **66**, 1501–1523, 1976.

GILBERT, J. F., Excitation of the normal modes of the Earth by earthquake sources, *Geophys. J. R. Astron. Soc.*, **22**, 223–226, 1970.

HARKRIDER, D. G., Surface waves in multilayered elastic media. I. Rayleigh and Love waves from buried sources in a multilayered elastic half-space, *Bull. Seismol. Soc. Am.*, **54**, 627–679, 1964.

HARKRIDER, D. G., Surface waves in multilayered elastic media. II. Higher mode spectra and spectral ratios from point sources in plane layered Earth models, *Bull. Seismol. Soc. Am.*, **60**, 1937–1987, 1970.

JORDAN, T. H. and P. G. SILVER, Parameters of normal-mode multiplets and their relationship to lateral heterogeneity, *EOS, Trans. Am. Geophys. Union*, **62**, 336, 1981 (abstract).

KANAMORI, H., Mechanism of tsunami earthquakes, *Phys. Earth Planet. Inter.*, **6**, 346–359, 1972.

KANAMORI, H. and J. J. CIPAR, Focal process of the great Chilean Earthquake of May 22, 1960, *Phys. Earth Planet. Inter.*, **9**, 128–136, 1974.

KANAMORI, H. and J. F. GIVEN, Use of long-period surface waves for fast determination of earthquake source parameters, *Phys. Earth Planet. Inter.*, **27**, 8–31, 1981.

MORIGUCHI, S., K. UDAGAWA, and S. HITOTSUMATSU, *Mathematical Formulae*, Vol. 3, *Special Functions*, Iwanami Publ. Co., Tokyo, 1959.

OKAL, E. A. and R. J. GELLER, On the observability of isotropic seismic sources: The July 31, 1970 Colombian Earthquake, *Phys. Earth Planet. Inter.*, **18**, 176–196, 1979.

ROMANOWICZ, B. A., Moment tensor inversion of long-period Rayleigh waves: A new approach, *J. Geophys. Res.*, submitted, 1981.

SAITO, M., Excitation of free oscillations and surface waves by a point-source in a vertically heterogeneous earth, *J. Geophys. Res.*, **72**, 3689–3699, 1967.

SHIMAZAKI, K. and P. SOMMERVILLE, Static and dynamic parameters of the Izu-Oshima Earthquake of Jan. 14, 1978, *Bull. Seismol. Soc. Am.*, **69**, 1343–1378, 1979.

SPAETH, M. G. and S. C. BERKMAN, The tsunami of Mar. 28, 1964 as recorded at tide stations, *in The Prince William Sound, Alaska Earthquake of 1964 and Aftershocks*, Vol. 2, Part B, pp. 223–307, U.S.G.S.E.S.S.A. Publ. 10-3, 1969.

STUMP, B. W., Investigation of seismic sources by the linear inversion of seismograms, 273 pp., Ph. D. Thesis, University of California, Berkeley, 1978.

WARD, S. N., Relationships of tsunami generation and in earthquake source, *J. Phys. Earth*, **28**, 441–474, 1980.